MULTIWAVELENGTH OBSERVATIONS OF THE AM HERCULIS TYPE SYSTEM: MR SERPENTIS[1]

J. Echevarría[2] , A. Schwarzenberg-Czerny[3,4], D.H.P. Jones[5], J.S.B. Dick[5],

M. Ward[6,7], R. Costero[2], and R. Gilmozzi[8,9]

RESUMEN

Se describen observaciones simultáneas en el ultravioleta y óptico así como otras observaciones de MR Ser durante un estado activo. No se detecta ninguna polarización lineal substancial durante un ciclo orbital; sin embargo, la polarización circular es muy intensa. El espectro ultravioleta muestra líneas intensas de N V λ1240, Si IV λ1400, C IV λ1550 y He II λ1640, típicas de otros sistemas tipo AM Her; adicionalmente presenta líneas semiprohibidas de N IV] λ1486, O III] λ1663 y N III] λ1750, no detectadas previamente en objetos similares. Un análisis de las condiciones físicas en las que se presentan estas líneas indica que la región emisora tiene una densidad típica de 10^{10} cm^{-3} y una temperatura de alrededor de 20 000 K. Las observaciones muestran que las líneas de H y He están autoabsorbidas y sufren fuertes efectos colisionales. La distribución de flujo desde el *UV* al *IR* se ajusta bien a una ley de potencias con índice $\approx -3/2$. Se compara la distribución en el óptico con la emisión ciclotrónica esperada para los objetos tipo AM Her. Las efemérides orbitales del objeto se revisan, encontrándose un período de 0.0788698 ± 0.000005 días.

ABSTRACT

We describe simultaneous ultraviolet and optical, as well as other observations of MR Ser during a high state. No substantial linear polarization was observed during an orbital cycle, but the circular polarization was high. The ultraviolet spectrum presents strong lines in emission of N V λ1240, Si IV λ1400, C IV λ1550 and He II λ1640, typical of other AM Her systems, and also shows semi-forbidden lines of N IV] λ1486, O III] λ1663 and N III] λ1750, not detected previously in similar objects. An analysis of the physical conditions in which these lines are produced, indicates that the emitting region has a typical density of about 10^{10} cm^{-3} and a temperature of about 20 000 K. The observations show that the H and He lines are self-absorbed, with relative intensities modified by collisions. The flux distribution from the *UV* to the *IR* is well fitted to a power law of index $\approx -3/2$. We compare the optical emission with that expected from cyclotron emission in AM Her objects. The orbital ephemeris are revised, and an improved period of 0.0788698 ± 0.000005 days is found.

Key words: **POLARIZATION – STARS-AM HER SYSTEMS – SPECTROPHOTOMETRY – ULTRAVIOLET SPECTRA**

I. INTRODUCTION

MR Ser (= PG1550+191) is a member of the AM Her class, a subgroup of cataclysmic variables. Reviews have been published by Chiappetti, Tanzi, and Treves (1980), Córdoba and Mason (1982), Liebert and Stockman (1985) and Cropper (1988). The AM Her stars consist

of a magnetic white dwarf accreting matter from a Roche-Lobe-filling red dwarf. The strong magnetic field (B $\approx$ a few 10^7 Gauss) inhibits the formation of a disc and channels the matter through one or both of the magnetic poles.

MR Ser was detected in the Palomar Green Survey by Green *et al.* (1982) and discovered to be an AM Her system by Stockman *et al.* (1981). Observations by Liebert *et al.* (1982) showed the presence of strong circular polarization and weak linear polarization pulses. The 0.078873-day orbital period derived from the linear pulse is also seen in optical light curves and radial velocity variations. Spectrophotometry by Echevarría, Jones, and Costero (1982) showed the presence of TiO bands associated with an M dwarf. Mukai and Charles (1986), have refined the spectral classification to a M5.5 V star, based on CCD spectroscopy. The object has been detected as a soft X-ray emitter using the EXOSAT low energy tele-

scope (Watson 1986). Ultraviolet spectroscopy shows a steep continuum distribution with possibly a hot Rayleigh-Jeans component (Szkody, Liebert, and Panek 1985). Photographic observations reported by Romano (1983) for the years 1972-1981, and photometry in 1982 made by la Dous and Schoembs (1987) reveal a regular variation in brightness from $V = 14.7$ to $V = 15.7$ Since July 1984 (Voíkhanskaya 1985) the system has gone into a low state ($V \approx 17$). Radial velocity observations in the near-infrared show evidence of chromospheric emission from the secondary star even during the low state (Mukai and Charles 1987). The observations reported in this paper were made before the system went into a low state.

II. OBSERVATIONS

The observations reported here were obtained using several different facilities and are summarized in Table 1.

a) *Photometry and Polarimetry*

Photoelectric photometry at *UBVRI* (Johnson) wavelengths was obtained with the No. 1 Pulse Counter Photometer attached to the 2.12-m telescope of the Observatorio Astronómico Nacional at San Pedro Mártir (SPM), Baja California, México. The integration time was 10 sec for each filter.

Simultaneous optical photometry and polarimetry

was obtained with the 3.8-m United Kingdom Infrared Telescope (UKIRT) on Mauna Kea, using the Hatfield polarimeter (Bailey and Hough 1982) in a configuration described by Bailey *et al.* (1983). Only the *V* filter observations are reported here.

Linear and circular polarization measurements in white light (extended S20 response) were obtained with the RGO two-channel travelling photometer attached to the 1.5-m Infrared Flux Collector (IRFC) on Tenerife, Islas Canarias, Spain. The polarimeter used was identical to that described in Jones, Smith, and Wallace (1981) with the exceptions that a quarter-wave plate was used to enable all four Stokes parameters to be obtained and the rotation period of the waveplate was constant at 960 msec with data collection in 20 msecs bins. The instrumentation computer used was an LSI 11/02 based system (Dick 1983), which provided real-time control of the CAMAC resident hardware, kept the astronomer informed of the progress of the observations, and printed the output which was also recorded on floppy disks.

b) *Ultraviolet and Optical Spectra*

Ultraviolet observations were made with the International Ultraviolet Explorer (IUE) monitored from the tracking station at Villafranca del Castillo, Madrid, Spain. Two low resolution short wavelength spectra were taken through the large aperture. The spectra were reduced using the IUE4 software package, available at the STAR-

TABLE 1

JOURNAL OF OBSERVATIONS OF MR SER

Spectroscopy							
Date	UT mid-exp. H	UT mid-exp. M	Exposure time (sec)	Wavelength range (A)	Detector, frame and observatory		
03AUG81	05	47	4320	3600 – 5600	OMA	T11-SP485	SPM
04AUG81	05	57	3240	3600 – 5600	OMA	T11-SP493	SPM
13AUG82	21	51	12000	1200 – 1950	SWP	17677	IUE
13AUG82	18	20	1200	3200 – 7200	RPCS	T99-64	SAAO
13AUG82	18	41	1200	3200 – 7200	RPCS	T99-65	SAAO
16AUG82	17	50	1200	3200 – 7200	RPCS	T99-176	SAAO
16AUG82	18	13	1200	3200 – 7200	RPCS	T99-177	SAAO
17AUG82	01	00	25000	1200 – 1950	SWP	17714	IUE

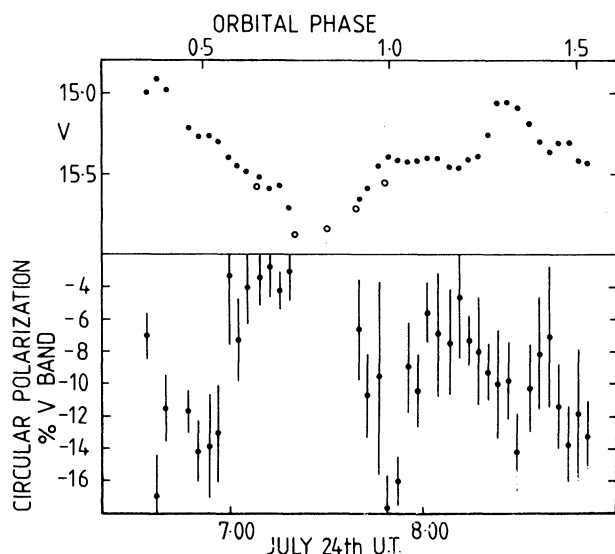| Photometry and Polarimetry					
Date	UT Start H	UT Start M	UT End H	UT End M	Wavelength coverage	Observing site
24JUL 82	07	08	07	48	*UBVRI*	SPM
24JUL 82	06	34	08	51	*V*	UKIRT
26MAY82	21	46	00	16	White	IRFC

Fig. 1. Simultaneous V light curve and circular polarimetry obtained at UKIRT, on 1982 July 24. Open circles are simultaneous V measurements from SPM.

LINK/VAX computer node at the Institute of Astronomy, Cambridge.

Optical spectra were obtained simultaneously with IUE using the 1.9-m telescope at the South African Astronomical Observatory (SAAO), with the Reticon Photon Counting System (RPCS) attached to the Unit spectrograph. A dispersion of 210 A mm^{-1} with a slit of 4.5 X 10 arcsec oriented EW gave a spectral resolution of about 8 A. The spectrophotometric standards LTT 7987 and LTT 9491 (Stone and Baldwin 1981) were observed in the same nights. A Cu-Ar lamp provided the wavelength calibration.

Optical spectra were also obtained with the 2.12-m telescope at SPM, using the Optical Multichannel Analyser described by Firmani and Ruiz (1981), attached to a Boller and Chivens spectrograph. The 200 lines mm^{-1} grating provided a 4 A per pixel resolution in its second order. The entrance slit of 3 X 165 arcsec permitted all the light to pass through and gave an estimated spectral resolution of 25 A; a second slit 7 arcsec east was used for sky subtraction. The spectrophotometric standard BD+40°4032 (Stone 1977) was observed on the same nights. A He-Ar lamp provided the wavelength calibration.

All of these optical spectra were reduced using the SPICA software package, available on the STARLINK/VAX computer node at the Royal Greenwich Observatory.

III. RESULTS

a) *Photometry*

The V light curve from UKIRT is shown in Figure 1, and is similar to the V light curves published by Liebert

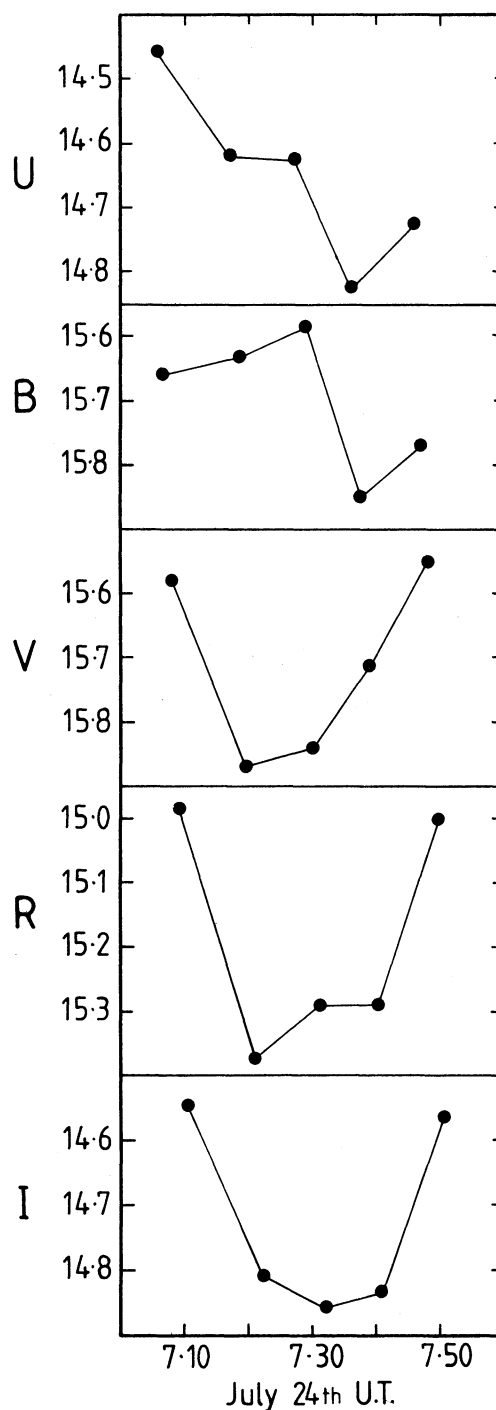Fig. 2. *UBVRI* photometry from SPM simultaneous to the data in Figure 1 during the broad eclipse.

et al. (1982) (henceforth LEA) and la Dous and Schoembs (1987), (the latter obtained simultaneously with our IUE and SAAO spectra). The V magnitude varies from 14.9 to 15.9, close to the values found by these authors and by Romano (1983). Figure 2 shows the *UBVRI* photometry obtained at SPM, simultaneously with UKIRT
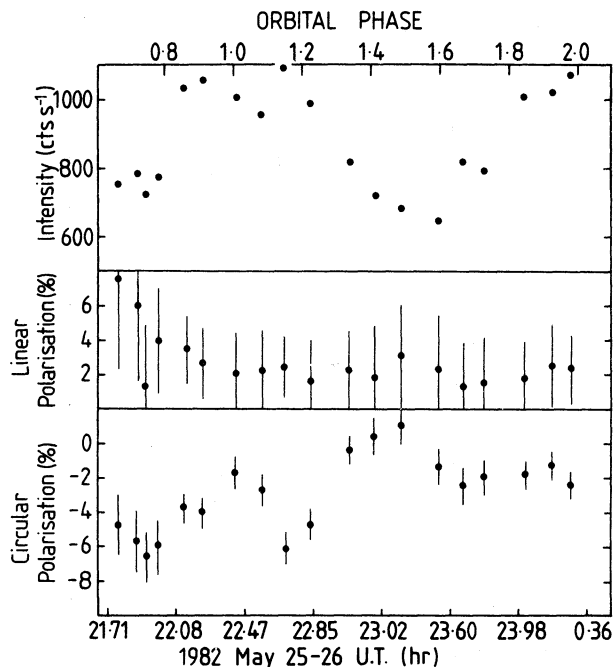
Fig. 3. Linear and circular polarization measurements obtained at IRFC on 1982 May 25-26. The observations were made in 'white light', i.e., the response of an unfiltered EMI 9658 photomultiplier.

and during the broad minimum. The same V magnitudes are shown in Figure 1. The broad minimum in the U and B bands shows a phase lag relative to the V observations. At longer wavelengths the minimum is broader.

Similar behavior is presented in Figure 3 from LEA. Figure 3 shows the white light curve obtained at IRFC. A shallow dip at phase 0.1 is present in all the light curves.

b) *Polarimetry*

The circular polarization in the V band measured at UKIRT (Figure 1) has a minimum of about -16 percent. Although we observe a maximum of about -5 percent at phase 0.2 (as defined by the ephemeris discussed in § IV), the polarization maximum is at phase 0.7, compared with LEA's maximum at 0.5 and does not reach zero. The IRFC polarization data is shown in Figure 3. No substantial linear polarization was observed except at phase 0.7. However, this feature does not reappear a cycle later. Two maxima are present in the circular polarization, but at phase 0.5 only does the circular polarization reach zero. Otherwise the agreement between the IRFC, UKIRT and LEA data is poor. These differences may arise from the use of different wavebands or may be due to intrinsic variations in the accretion parameters, e.g., in the mass transfer rate.

c) *Ultraviolet and Optical Spectroscopy*

The SWP observation on August 17 is shown in Figure 4. We have identified strong emission features of N V λ1240, Si IV λλ1393, 1402, C IV λ1550 and He II λ1640 and weak C II λ1335. Also present are the semiforbidden lines of N IV] λ1486, O III] λ1663 and N III] λ1750. These lines are also present in the scan of August 14, not shown in the figures. Since these intercombination lines are present in the spectra, it is possible that O IV] λ1402 contributes substantially to the Si IV line.

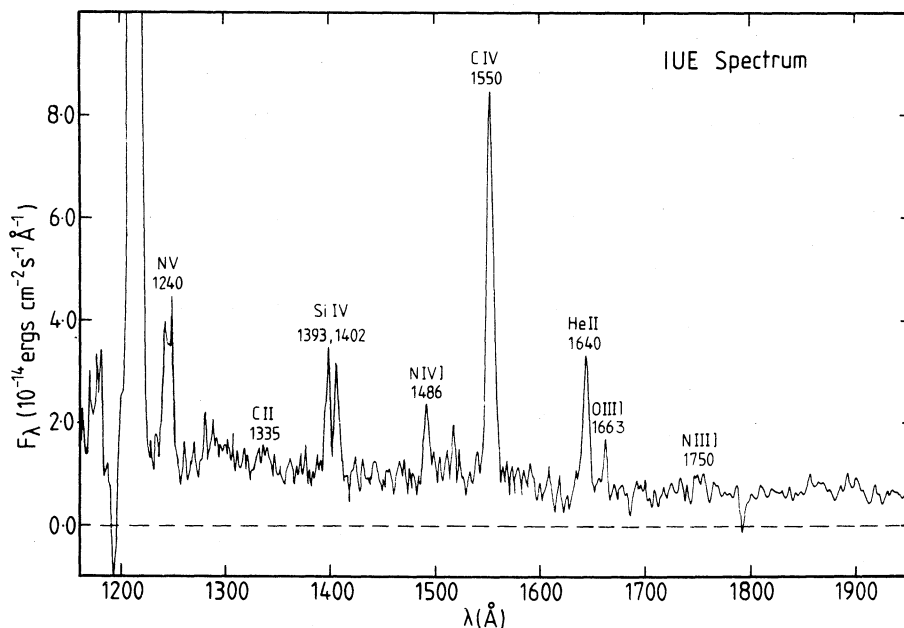Fig. 4. Ultraviolet shortwave spectrum obtained with IUE on 1982 August 17.

TABLE 2

ULTRAVIOLET LINE INTENSITIES RELATIVE TO Hβ

Line Identification	λ (A)	F (λ)/F (Hβ)[a]	f (λ)	I (λ)/I (Hβ)
N V	1240	6.65	1.639	8.66
C II	1335	1.00	1.416	1.26
Si IV	1393	3.00	1.318	3.71
Si IV + O IV] ?	1402	2.88	1.307	3.56
N IV]	1486	2.39	1.230	2.91
C IV + C IV	1548, 51	10.91	1.183	13.20
He II	1640	3.80	1.136	4.56
O III]	1663	1.93	1.129	2.32
N III]	1750	1.00	1.119	1.20

a. F (Hβ) from SAAO spectra.

The emission line intensities relative to Hβ (measured simultaneously at SAAO) are shown in Table 2. The mean of the two spectra obtained at SPM are depicted in Figure 5. This shows strong Hydrogen and He II lines; moderately strong He I lines in addition to weak lines of Carbon, Nitrogen, Calcium and Iron. The emission line fluxes are presented in Table 3. The mean of the four spectra obtained at SAAO is illustrated in Figure 6. This shows a similar degree of ionization as the SPM spectra. At shorter wavelengths permitted oxygen lines are detected. The emission line fluxes are given in Table 3. The sky emission lines are not well subtracted and are flagged with an S. Since no blocking filters were used with the spectrograph, the continuum around 7000 A is contaminated by the blue continuum of the next order.

Line intensities I(λ) corrected for interstellar absorption were calculated using the relation

$$\log I(\lambda)/I(H\beta) = \log F(\lambda)/F(H\beta) + C(H\beta) f(\lambda) \qquad (1)$$

where F(λ) is the observed flux corrected for atmospheric extinction, C(Hβ) is the logaritmic reddening function and f(λ) is the reddening function normalized at Hβ, derived from the normal extinction law (Seaton 1979). A rough estimate of C(Hβ) can be made based on the distance to MR Ser. We proceed as follows: assuming a distance of 150 pc from Mukai and Charles (1987), an average value for the extinction A_V of 1 mag kpc^{-1} and $A_V/E(B - V) = 3.2$. If C(Hβ) = 1.47E($B - V$) (Seaton 1979), then E($B - V$) = 0.05 and C(Hβ) = 0.07. Szkody et al. (1985) estimate E($B - V$) $\leqslant$ 0.1, consistent with the previous result. C(Hβ) could also be derived from the He II ratio λ1640/λ4686, if this ratio were produced by recombination and the temperature and density were known. However, we will show in §V that this is probably not the case.

A comparison of the SPM spectra from 1981 with the SAAO spectra from 1982 reveals several differences. The greater width of the emission lines at SPM is readily explained by the lower resolving power of the Boller & Chivens spectrograph. However, the line intensities in 1981 are at least twice as high as in 1982, and we believe this effect to be real.

Variations of a factor of ten in the Balmer lines have been observed by Maraschi et al. (1984) in the similar AM Her variable, V834 Cen. Moreover, the continuum flux in both spectra are $F_\lambda \approx 1.5 \times 10^{-15}$ ergs cm^{-2} s^{-1} A^{-1} from 4000 to 5400 A, which suggests that the spectro-
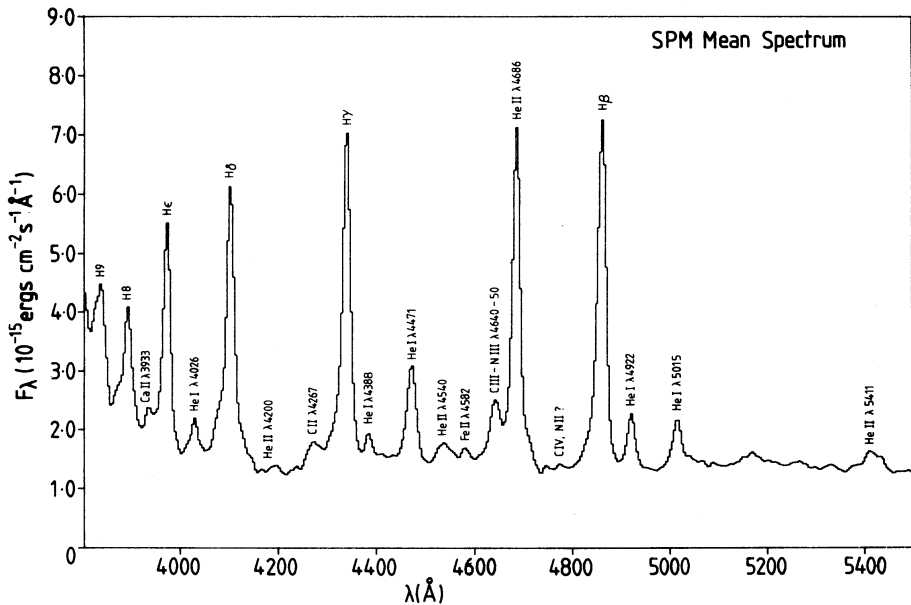

Fig. 5. Mean optical spectrum from SPM observations on 1981 August 3 and 4.

TABLE 3

OPTICAL EMISSION LINE INTENSITIES RELATIVE TO Hβ

Line Identification	λ (A)	F (λ)/F (Hβ) SPM	F (λ)/F (Hβ) SAAO	f (λ)	I (λ)/I (Hβ) SPM	I (λ)/I (Hβ) SAAO
O III	3429	...	0.11	0.343	...	0.12
O III, He I	3444, 48	...	0.13	0.337	...	0.14
He I	3614	...	X 0.02	0.287	...	≤ 0.03
He I, O III	3705, 12	...	0.14	0.261	...	0.15
H11, He II	3770	...	0.20	0.245	...	0.22
H10, He II	3798	...	0.26	0.239	...	0.27
H9, He I, He II	3835	0.21	0.41	0.231	0.22	0.43
H8, He I, He II	3889	0.26	0.51	0.219	0.27	0.53
Ca II	3933	0.03	0.19	0.210	0.03	0.20
Hε, He I, He II	3970	0.48	0.71	0.201	0.50	0.73
He II, He II	4026	0.08	0.15	0.190	0.08	0.15
Hδ, He II	4101	0.78	0.68	0.171	0.80	0.70
He I	4120	...	≤ 0.03	0.167	...	≤ 0.03
He I	4144	...	≤ 0.05	0.163	≤ 0.05	≤ 0.05
He II	4200	0.06	≤ 0.03	0.152	0.06	≤ 0.03
C II	4267	0.06	0.09	0.141	0.06	0.09
Hγ, He II	4340	0.86	0.84	0.128	0.88	0.86
He I	4388	0.04	0.09	0.117	0.04	0.09
He I	4471	0.26	0.33	0.095	0.27	0.34
He II	4541	0.11	0.09	0.076	0.11	0.09
Fe II	4584	0.02	0.02	0.065	0.02	0.02
C III, N III	4640-50	0.18	0.18	0.052	0.18	0.18
He II	4686	0.90	0.86	0.041	0.91	0.87
He I	4713	...	0.06	0.035	...	0.06
Hβ, He II	4861	1.00	1.00	0.000	1.00	1.00
He I	4922	0.12	0.19	−0.014	0.12	0.19
He I	5016	0.11	0.18	−0.035	0.11	0.18
He I	5047	...	0.04	−0.043	...	0.04
He II	5411	0.08	0.11	−0.117	0.08	0.11
He I	5876	...	0.42	−0.217	...	0.41
Hα, He II	6563	...	0.87	−0.323	...	0.83
He I	6678, 83	...	0.18	−0.337	...	0.17
He I	7065	...	0.09	−0.383	...	0.08
log F (Hβ)[a]		−12.88	−13.11	...	...	...
C (Hβ)		0.07	0.07	...	...	...
log I (Hβ)[a]		...	...	...	−12.81	−13.04

a. ergs cm^{-2} s^{-1} .

photometry in this region has errors of less than about 10 percent. Nevertheless, the two spectra are badly discrepant in flux at wavelengths shorter than λ4000 A, where the SAAO spectrum is systematically weaker. We believe that this is due to a stronger Balmer jump in emission in 1981 but may also be partially due to the fact that the SAAO spectra suffer from stronger atmospheric dispersion (minimum zenith distance 50°) than the SPM spectra (minimum zenith distance 10°), carrying the ultraviolet flux out of the aperture. The SAAO spectrum has stronger He I lines than the SPM spectra. λ4471 is 70 percent stronger and line blends such as H8+He 1 and Hε+He I become dominated by the He I component. We also detect weak He I lines, like λ4713 and λ5047, not present in the SPM spectra. The He II and Balmer line ratios are nearly the same in both spectra.

IV. THE EPHEMERIS

LEA presented an ephemeris for the occurrence of the linear polarization peaks, based on observations from the 1981 season. They find an orbital period of 0.078873 day. Their ephemeris should be sufficiently accurate to determine the phases of our 1982 observations ± 0.06. We have no linear polarization measures of sufficient quality to confirm the accuracy of the LEA ephemeris. However, our photometric data combined with LEA and la Dous and Schoembs (1987) observations, could be used to derive an improved ephemeris, assuming the polarimetric and photometric periods to be the same. LEA's centres of broad light minima correspond to the polarimetric phase 0.6 (their Figure 3). We assume synchronic rotation as in all other polars and use this phase for our optical minima. The observed
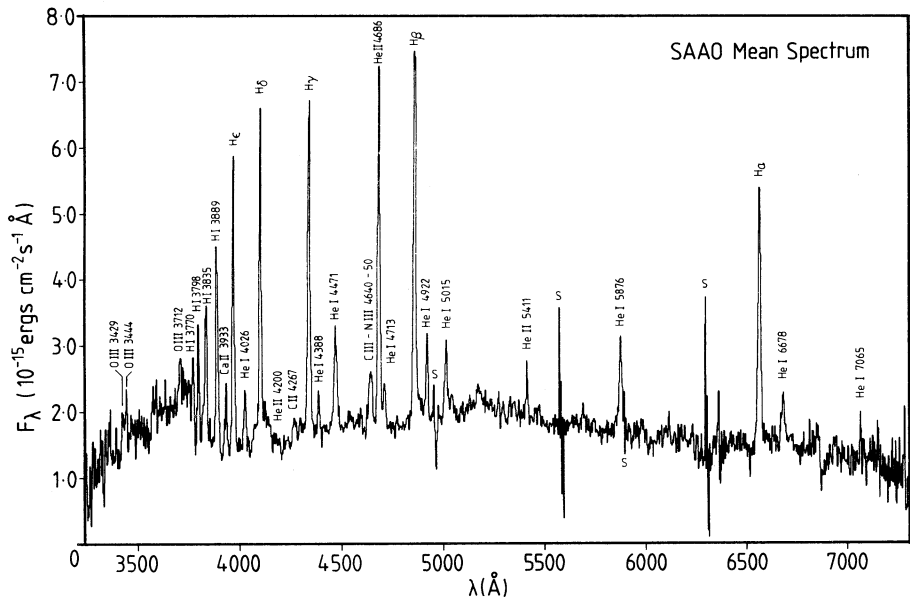
Fig. 6. Mean optical spectrum from SAAO observations obtained on 1982 August 13 and 16.

light minima and linear polarization maxima are listed in Table 4. Light minima are much broader than linear polarization maxima, so random errors in their times are expected to be greater. The mean of the periods derived from the 1981 and 1982 epochs is sufficiently accurate to establish a unique cycle count for all these data. In particular, the 1982 July 24 observation is suitable placed to dismiss any possibility of miscounting the number of cycles. The improved ephemeris obtained by a least squares fit to all data is given by:

$$HJD = 2444853.1973 + 0.0788698(E-1134). \quad (2)$$

$$\pm 0.0010 \pm 0.000005$$

This corresponds to the linear polarization spike. The errors in epoch and period are uncorrelated because of our choice of central epoch. The O−C phases in Table 4 show that our calculated ephemeris yields smaller errors for all observations. Mukai and Charles (1987) have also re-analysed the ephemeris of MR Ser using the radial velocity information from LEA and Voikhanskaya (1985). They suggest two possible new values for the orbital period: 0.0788693 and 0.0788749. They adopt the latter value following Cropper's polarization (unpublished). The first value is in close agreement with our ephemeris. Mukai and Charles (1987) have also calculated $P = 0.07887 \pm 0.00010$ days based on their own radial velocity observations derived from the Na II absorption doublet. This value is also closed to our adopted period.

V. THE EMISSION LINE REGION

The emission lines in AM Her systems arise from sev-

TABLE 4

DEPARTURES FROM EPHEMERIS

HJD 2444700+ Lin. pol. pulse	E	ϕ_1 (O − C)[a] LEA	ϕ_2 (O − C)[a] This paper
63.76025	0	0.02	0.02
64.70508	12	0.00	0.00
65.72998	25	−0.01	−0.01
66.67578	37	−0.02	−0.02
66.75635	38	0.00	0.00
67.69971	50	−0.03	−0.03
68.73535	63	0.10	0.10
69.75098	76	−0.03	−0.03
70.69580	88	−0.05	−0.05
78.66846	189	0.03	0.04
79.84375	204	−0.07	−0.06
146.65527	1051	0.01	0.05

Broad light min.

415.482	4459.6	−0.25	−0.07
474.803	5211.6	−0.13	0.08
498.376	5510.6	−0.26	−0.04

a. ϕ_1 is calculated from the ephemeris of LEA and ϕ_2 from our ephemeris given in the text.

eral distinct zones as discussed by several authors (c.f. Liebert and Stockman 1985 and references therein). In the optical range they have at least two components: a broad emission base which is usually very strong, and a narrow component whose velocity variations lag behind those of the broad component in phase. In MR Ser the broad and narrow flux components are comparable. Moreover, the similarity of the systemic velocity derived

by LEA for the H, He I and He II lines, suggests that they are produced in the same region. Liebert and Stockman (1985) favour a scenario in which the narrow emission lines are produced in the chromosphere of the red dwarf, in a region between the inner Lagrangian point and the surface of the red dwarf. This view is supported by the radial velocity observations of the Ca II triplet emission in the near-infrared by Mukai and Charles (1987). They find that these lines are produced in the chromosphere of the red star even during a low state. Since the *UV* spectra cannot be phase-resolved, it is not possible to determine the location of the *UV* lines. We will simply assume that they are formed in the same region as the optical narrow line components.

The presence of the semi-forbidden emission lines in the ultraviolet imply densities of $N_e \leqslant 10^{11}$ cm^{-3} since they are collisionally de-excited above this limit. In particular the N IV] $\lambda 1486$ line sets an upper limit of $N_e \leqslant 3.16 \times 10^{10}$ (Ferland *et al.* 1982). On the other hand, the absence of any forbidden lines in the optical spectrum requires $N_e \geqslant 10^8$ cm^{-3}. Furthermore, the absence of C III $\lambda 1909$ may be explained if the electronic density is above the critical density of this line, $N_e \geqslant 9 \times 10^9$ cm^{-3} (obtained from the collision strengths and spontaneous emission coefficients tabulated in Mendoza 1983). However, as pointed out by Ferland *et al.* (1982) for the case of V603 Aql, an old nova with a similar *UV* spectrum, it is more likely that there is very little C^{+2} in the emission region since the N IV] line is quite strong.

Further limits on the electronic temperature and density may be found by examining the physical conditions in which the H and He lines are produced. Since all Balmer lines are blended with He I and He II lines, we have examined them carefully in order to assess the individual contributions (see Table 5). Although we will argue that

TABLE 5

OBSERVED AND PREDICTED BALMER RATIOS

	$I(\lambda)/I(4861)$						
λ	(1)	(2)	(3)	(4)	(5)	(6)	(7)
6563	0.78	0.54	2.70	1.85	3.08	1.61	0.56
4340	0.88	0.73	0.49	0.73	0.54	0.73	1.20
4101	0.72	0.68	0.29	0.62	0.37	0.60	1.30
3970	0.76	0.67	0.19	0.55	0.30	0.53	1.36
3889	0.55	$\leqslant 0.55$	0.13	0.50	0.26	0.49	1.40
3835	0.44	0.35	0.10	...	0.26	0.49	1.45
3798	0.28	0.27	0.07	...	0.22	0.44	1.45
3770	0.22	0.21	0.06	...	0.21	0.43	1.46

(1) SAAO Observations. (2) SAAO with He contributions subtracted (see text). Hummer and Storey (1987) Case B; (3) $T_e = 3 \times 10^3$ K, $N_e = 10^{11}$ cm^{-3}. Drake and Ulrich (1980) Hydrogen at moderate and high densities. (4) Model i): $T_e = 2 \times 10^4$, $N_e = 3 \times 10^{12}$, $\tau(L\alpha) = 10^5$, $R_{1c} = 3 \times 10^{-2}$. (5) LTE limit for $T_e = 3300$ K. (6) LTE limit for $T_e = 4600$ K. (7) LTE limit for $T_e = 1.5 \times 10^4$ K.

TABLE 6

OBSERVED AND PREDICTED He II LINE RATIOS[a]

	$I(\lambda)/I(4686)$			
λ	SAAO	(1)	(2)	(3)
6560	Blend	0.160	0.153	0.155
5411	0.12	0.120	0.112	0.118
4859	Blend	0.0997	0.0886	0.0934
4541	0.10	0.0908	0.0765	0.0730
4339	Blend	0.0873	0.0693	0.0561
4200	$\leqslant 0.03$	0.0826	0.0622	0.0431
4100	Blend	0.0734	0.0538	0.0334
1640	5.24	8.69	8.89	9.40

a. Hummer and Storey (1987) Case B. (1) $T_e = 5 \times 10^3$ K; $N_e = 10^{11}$ cm^{-3}. (2) $T_e = 1 \times 10^4$ K; $N_e = 10^{11}$ cm^{-3}. (3) $T_e = 3 \times 10^4$ K; $N_e = 10^{12}$ cm^{-3}.

neither Case B recombination nor the inclusion of large optical depths or collisional de-excitation can accurately reproduce the observations; at least in the optical range some line ratios are similar to their recombination values. Hα is blended with He II $\lambda 6560$, whose contribution could be as high as 0.14, relative to Hβ, as judged from the comparative theoretical values in Table 6 and discussed below. Contributions of the He II lines to Hβ and Hγ are easier to derive since we can interpolate directly from neighbouring He II lines. Hβ and Hγ have a contribution of 0.09 from He II $\lambda 4859$ and 0.04 from He II $\lambda 4100$ respectively. The He II contamination to other H lines is $\leqslant 0.03$. Hδ, H8 and H9 are blended with the He I lines $\lambda 3964$, $\lambda 3889$ and $\lambda 3820$ respectively. The contribution of $\lambda 3964$ is expected to be about 1/3 the intensity of $\lambda 5016$ (see below and Table 7), while $I(\lambda 3820)$ should be around 1/2 of $I(\lambda 4026)$. The intensity of $\lambda 3889$ is not easy to estimate. At low densities and negligible optical depths it could be as high as 0.9 relative to Hβ, as seen for Case A in Table 7 (which is incompatible with the observed (H8+He I/Hβ ratio). For large optical depths in the 2^3S-n^3P transitions, the intensity of $\lambda 3889$ decreases rapidly while $\lambda 7065$ is enhanced by resonance fluorescence (Osterbrock 1974). This is also incompatible with the observed strength of $\lambda 7065$. On the other hand, as pointed out by Osterbrock (1974), it is likely that collisional excitation alone will affect the strength of $\lambda 3889$. In a region of medium density and high optical depths in the triplet lines, $\lambda 3889$ will not contribute substantially to H8.

In Table 5 we compare the observed Balmer line ratios with theoretical calculations for densities in the range 10^{11} to 10^{15} cm^{-3}. Column (1) shows the SAAO observations (comparison is not given with the SPM data because of non-simultaneity with IUE). The corrected line fluxes from He contributions discussed above are given in column (2). Results from Hummer and Storey (1987) for Case B recombination are given in column (3) for

TABLE 7

OBSERVED AND PREDICTED He I LINE RATIOS[a]

Singlet Lines I (λ)/I (4922)				Triplet Lines I (λ)/I (4471)		
λ	SAAO	(1)	(2)	λ	SAAO	(2)
$2^1P - n^1D$				$2^3P - n^3S$		
6678	0.84	2.80	2.80	7065	0.24	0.32
4388	0.47	0.47	0.47	4713	0.18	0.09
4144	⩽0.26	0.26	0.26	4120	⩽0.09	0.04
$n^1S - 2^1P$				$2^3S - n^3P$		
5047	0.21	0.14	0.10	3889	Blend	2.29
$n^1P - 2^1S$				$2^3P - n^3D$		
5016	0.95	2.15	0.05	5876	1.15	2.69
3964	Blend	0.87	0.03	4026	0.47	0.48
3614	⩽0.16	0.43	0.02	3820	Blend	0.27
3448	Blend	0.24	0.01	3705	Blend	0.16

a. Brocklehurst (1971). (1) Case B; $T_e = 10^4$ K; $N_e = 10^7$ cm^{-3}. (2) Case A; $T_e = 10^4$ K; $N_e = 10^7$ cm^{-3}.

$T_e = 2 \times 10^4$ K and $N_e = 10^{11}$ cm^{-3}. Column (4) shows some of the results by Drake and Ulrich (1980) for a slab of hydrogen at moderate densities for Model i: $T_e = 2 \times 10^4$ K, $N_e = 10^{11}$ cm^{-3}, τ (Lα) = 10^5 and $R_{1c} = 3 \times 10^{-2}$, where τ (Lα) is the optical depth of Lα and R_{1c} is the value of the ground-state photoionization rate. Finally, columns (5) to (7) give the high density limit or LTE values for the Balmer lines adopted from Drake and Ulrich (1980). The observations differ from Case B values in that Hα has an inverted decrement (which is typical of other cataclysmic variables, e.g., Williams and Ferguson 1982), while the rest of the Balmer lines have unusually strong lines relative to Hβ. Thus the Case B model where collisional excitation is important does not fit the observations.

As pointed out by Drake and Ulrich (1980) there are three basic processes which can cause the Balmer decrement to deviate from Case B. The first is self-absorption, i.e., large optical depths in the Balmer lines, which causes a substantial increase in Hα/Hβ and a decrease in other Balmer line ratios relative to Hβ. The reason for this behaviour is that radiative decay from n = 3 level is reduced. This process can be important at low densities. Collisional excitation, the second one, produces a further increase in the Hα/Hβ ratio and a decrease in the Hn/Hβ ratios, because as the density increases collisional excitation contributes to the population of the n = 3 level. The third process, collisional de-excitation, the dominant mechanism at high densities, depopulates level 3 and therefore as the density increases, the ratio Hα/Hβ decreases towards its LTE value, while all the Hn/Hβ ratios increase. Numerous examples of the behaviour of the Balmer lines as a function

of temperature, density, optical depth and ground-state photoionization rates, may be found in the work referenced above. However, in no case do we find a low Hα/Hβ with the Hn/Hβ ratios decreasing as observed in MR Ser. A few examples are shown in Table 5. Drake and Ulrich's Model i in column (4) agrees with the Hn/Hβ values but also predicts a high Hα/Hβ ratio. In fact all medium density models predict Hα/H$\beta \geqslant 1.5$. Lower values can be obtained only at very high temperatures and densities as shown in column (7), but with the associated result of high Hn/Hβ ratios which are not observed in MR Ser. Low temperatures and very high densities can reproduce the observed Hn/Hβ ratios but again predict very large Hα/Hβ, as shown in the examples given in columns (5) and (6). We tend to favour a medium density zone for formation of the Balmer lines for two reasons: first, if the UV lines are produced in the same region as the H and He lines, then the electronic density has to be of the order of 10^{10} cm^{-3}; and second, as shown by Echevarría (1988), the Hn/Hβ ratios of cataclysmic variables with accretion discs are well correlated with temperature, while Hessman (1985) has demonstrated that this is not the case for Hα/Hβ. Furthermore, the LTE models by Drake and Ulrich (1980) reproduce very well the Hγ/Hβ and Hδ/Hβ observed temperature correlation. It is possible that Hα/Hβ requires a special non-LTE treatment (Hessman 1985). In any case, self-absorption of the Balmer lines of MR Ser is expected, together with densities of the order of 10^{11} cm^{-3}.

A larger number of He I lines are present in our spectra. The most important ones are compared in Table 7 with the standard recombination values from Brocklehurst (1982). These values are given for densities $N_e \leqslant 10^7$ cm^{-3}, which are lower than we expect. However, comparison is still instructive. For example, we note that $\lambda5016/\lambda4922$ has a ratio between Case A and B. In general the $n^1P - 2^1S$ transitions are very sensitive to optical depth because of the metastable 2^1P level. We believe that, contrary to this effect, emission from these singlet states is decreased by collisional excitation in a similar way to the Hn/Hβ lines. In fact this mechanism may apply to all first members of line series like $\lambda6678$, $\lambda5016$, $\lambda7065$ and $\lambda5876$ which also have inverted decrements.

The He II lines are also strong in MR Ser. In the optical, the Pickering lines are very conspicuous as judged from the uncontaminated lines at $\lambda5411$, $\lambda4541$ and $\lambda4200$. The strongest line, Paschen α $\lambda4686$ is comparable in strength with Hβ. In the ultraviolet range, Balmer α $\lambda1640$ is also very strong. These lines are compared in Table 6 with expected Case B values for three different cases. The closest agreement with the observations is given for $T_e = 5 \times 10^3$ K, chosen because it most nearly fits the optical lines and provides the smallest 1640/4686 ratio. Nevertheless, the observed intensity of $\lambda1640$ is too small to match any temperature calculations at densities $\geqslant 10^9$ cm^{-3}. It would be necessary to arbitrarily set C(Hβ) $\geqslant 0.25$ to produce a con-

sistent set of He II lines. But such a high extinction value is ruled out by the absence of any strong absorption in the 2200 A band (Szkody *et al.* 1985; Osborne 1983, private communication). An alternative explanation may be found if it is assumed that not only the He II Lyman lines are optically thick, but also the He II Balmer lines, because in this case $\lambda1640$ will have a lower flux compared with $\lambda4686$. If we compare the optical lines alone with Case B calculations, the best match is given for higher temperatures, between 10^4 and 3×10^4 K, and at densities of 10^{11} or 10^{12} cm^{-3}.

VI. CONTINUUM FLUX DISTRIBUTION

The continuum distribution of MR Ser is depicted in Figure 7. The ultraviolet observations from 1900 to 3200 A were kindly provided by Osborne (1983, private communication) and normalized to the SWP spectrum. The infrared magnitudes are from LEA. An interstellar reddening correction of $E(B - V) = 0.05$ was applied to the data, as discussed in §IIIc. Although the whole flux distribution cannot be fitted by a single power law, a good fit to the *UV*, optical and *IR* data is obtained for an index close to $-3/2$. The IUE data is similar to the spectra obtained by Szkody *et al.* (1985), taken 10 months after our SWP spectrum. Although there is an increase in flux for $\lambda \leqslant 1600$ A, the contamination from the terrestrial Lα and the strong N V line precludes an accurate estimate of the continuum in this region. If real, the turn-up is probably associated with the *EUV* component which is suspected to be present in these stars and which would arise from X-ray heating of the white dwarf in the neighbourhood of the magnetic poles, or by heating of the facing hemisphere of the red dwarf. The flux distribution at optical wavelengths alone is best fitted with a $F_\lambda \propto \lambda^{-2}$, except for $\lambda \leqslant 4500$ A shortward of which the flux decreases very rapidly. As indicated in §IIIc, this may be a real feature but it is also possible that the SAAO spectra have not been corrected sufficiently for strong atmospheric dispersion carrying the ultraviolet flux out of the aperture. If real, the decrease may be explained by the optical cyclotron emission as detected in other AM Her stars. Barrett and Chanmugan (1984) have predicted the polarization from cyclotron emission when collisions, and Thompson scattering are taken into account. These calculations predict polarizations comparable to those observed. It is therefore possible that the visible light is dominant by this mechanism. They have shown that it is no longer necessary to invoke the photospheric flux component which was required, because the earlier calculations predicted that light from cyclotron emission would be totally polarized. A further modification resulting from Barrett and Chanmugan's calculations is that the predicted cyclotron emission no longer drops off so rapidly towards the higher harmonics. In Figure 7 we have plotted the spectrum of cyclotron emission from harmonics 4 to 8 taken from Barrett and Chanmugan (1984) with the fol-
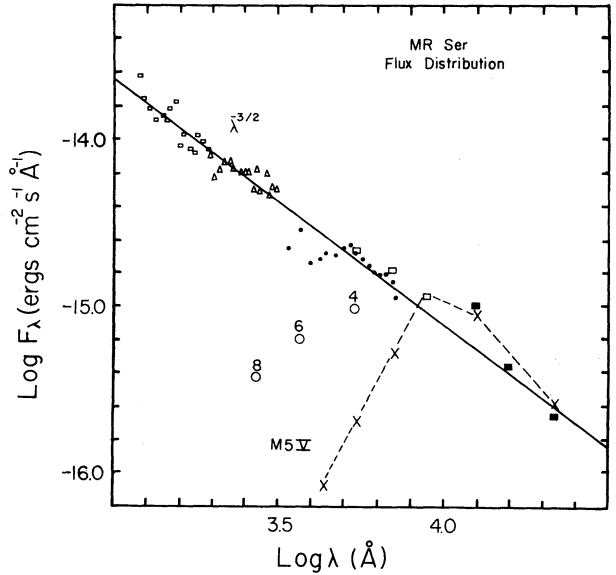

Fig. 7. Flux distribution of MR Ser. Small squares are ultraviolet SWP shortwave data, triangles are ultraviolet LWR longwave data (Osborne, private communication) corrected for $E(B - V)$ of 0.05. Dots are RPCS observations, large open squares are *V,R,I* from this paper, while large filled squares are *J,H,K* magnitudes from LEA. The dotted curve represents an M5.5 star. The straight line is a power law with index $-3/2$. The open circles labeled 4, 6 and 8 are the corresponding harmonics discussed in the text.

lowing parameters; $\alpha = 30°$, kT = 0.2 KeV, $\lambda_\beta = 22000$ A. This can be well fitted to our spectrum down to $\lambda3400$ A. The infrared colours show a slight shoulder at $\lambda12500$ A, probably resulting from the contribution of the M5.5 secondary. The flux distribution of a main sequence M5.5 star is also shown in Figure 7. We note that the overall flux distribution of MR Ser resembles that of V834 Cen (Maraschi *et al.* 1984).

VII. THE ACCRETION COLUMN

Barrett and Chanmugan (1984) have computed the flux and polarization for the same cyclotron emission parameters as a function of angle with the line of sight α. Qualitatively we can identify three separate phases:

a) $\alpha = 90°$; maximum linear polarization, zero circular, maximum flux.

b) $\alpha = 45°$; zero linear polarization, maximum circular polarization, intermediate flux.

c) $\alpha = 0°$; zero linear polarization, zero circular polarization, minimum flux.

We compare our Figures 1 and 3 with Figures 2 and 3 of LEA to identify these phases. By definition, phase zero coincides with the linear polarization pulse and we identify it with phase *a*. The circular polarization approaches zero although it does not vanish completely. Maximum light does not occur at phase zero but at

about phase 0.2. The absolute value of the circular polarization has two maxima in each cycle at phases 0.3 and 0.7. At both phases the linear polarization is negligible. Phase 0.3 occurs before minimum light and phase 0.7 after minimum so we can confidently identify both with phase *b*. The absolute value of the circular polarization falls to its overall minimum at phase 0.5, it is then vanishingly small. There is no linear polarization at this phase and the flux is at minimum. This must correspond to our phase *c*.

We are thus led to agree with LEA in claiming that we are observing only the South Magnetic Pole which always remains on the visible hemisphere of the white dwarf. During each rotation period of the white dwarf it moves from near the centre of the disc to near the limb (α 0 − 90°). For this to occur, both the inclination of the system and the latitude of the magnetic pole must be about 45°.

VIII. CONCLUSIONS

We have presented ultraviolet and optical observations of MR Ser during a high state. The results may be summarized as follows:

1) No substantial linear polarization was observed during an orbital cycle, but circular polarization is high. The position of the accretion column as a function of orbital phase, derived from the polarization is compared with the cyclotron polarized emission calculated by Barrett and Chanmugan (1984). This analysis supports the model put forward by LEA that the south pole accretion column remains visible throughout the rotation period of the magnetic white dwarf.

2) The ultraviolet spectrum shows semi-forbidden lines of N IV] λ1486, O III] λ1663 and N III] λ1750, not detected previously in similar objects. A comparison of *UV* and optical emission lines with theoretical models indicate that the emitting region has a typical density of about 10^{10} cm^{-3} and a temperature of about 2×10^4 K. The H and He lines are dominated by self-absorption and collisional processes.

c) The flux distribution from the *UV* to the *IR* is well fitted by a power law of index ≈ −2. We compare the optical emission with that expected from cyclotron emission in AH Her objects.

We are pleased to thank Drs. J.A. Bailey, D. Axon, F. Verbunt and M. Tapia for help with many aspects of

this paper, and especially to Drs. M. Peimbert and R. Williams for discussing with us the physics of the emission line region. We are also indebted to the staff of VILSPA, UKIRT, SAAO and SPM for their generous and valuable support.

REFERENCES

Bailey, J. and Hough, J.M. 1982, *Pub. A.S.P.*, **94**, 618.
Bailey, J. *et al.* 1983, *M.N.R.A.S.*, **205**, 1p.
Barrett, P.E. and Chanmugan, G. 1984, *Ap. J.*, **278**, 298.
Brocklehurst, M. 1972, *M.N.R.A.S.*, **157**, 211.
Chiappetti, L., Tanzi, E.G., and Treves, A. 1980, *Space Sci. Rev.*, **27**, 3.
Córdoba, F.A. and Mason, K.O. 1982, *Accretion Driven X-Ray Sources*, eds. W.H.G. Lewin and P.J. Heuvel (Cambridge: Cambridge University Press).
Cropper, M. 1988, *Proceedings of COSPAR/IAU Symposium on the Physics of Compact Objects: Theory vs. Observation*, ESA, Nordvijk/Paris.
Dick, J.S.B. 1983, D. Phil. Thesis, University of Sussex.
Drake, S.A. and Ulrich, R.K. 1980, *Ap. J. Suppl.*, **42**, 211.
Echevarría, J. 1988, *M.N.R.A.S.*, **233**, 513.
Echevarría, J., Jones, D.H.P., and Costero, R. 1982, *M.N.R.A.S.*, **200**, 23p.
Ferland. G.J. *et al.* 1982, *Ap. J.*, **260**, 794.
Firmani, C. and Ruiz, E. 1981, *Symposium on Recent Advances in Observational Astronomy*, eds. H.L. Johnson and C. Allen (México: Universidad Nacional Autónoma de México), p. 25.
Green, R.F., Ferguson, D.H., Liebert, J., and Schmidt, M. 1982, *Pub. A.S.P.*, **94**, 560.
Hessman, F.V. 1985, Ph. D. Thesis, University of Texas at Austin.
Hummer, D.G. and Storey, P.J. 1987, *M.N.R.A.S.*, **224**, 801.
Jones, D.H.P., Smith, F.G., and Wallace, P.T., 1981, *M.N.R.A.S.*, **196**, 943.
la Dous, C. and Schoembs, R. 1987, *Inf. Bull. Var. Stars*, No. 3068.
Liebert, J. *et al.* 1982, *Ap. J.*, **256**, 594.
Liebert, J. and Stockman, H.S. 1985, *Cataclysmic Variables and Low-Mass X-Ray Binaries*, eds. D.Q. Lamb and J. Patterson, (Dordrecht: D. Reidel), p. 151.
Maraschi, M. *et al.* 1984, *Ap. J.*, **285**, 214.
Mendoza, C. 1983, in *Planetary Nebulae, IAU Symposium No. 103*, ed. D.R. Flower (Dordrecht: D. Reidel), p. 143.
Mukai, K. and Charles, P.A. 1986, *M.N.R.A.S.*, **222**, 1p.
Mukai, K. and Charles, P.A. 1987, *M.N.R.A.S.*, **226**, 209.
Osterbrock, D.E. 1974, *Astrophysics of Gaseous Nebulae*, Freeman and Co.
Romano, G. 1983, *Inf. Bull. Var. Stars*, No. 2265.
Seaton, M.J. 1979, *M.N.R.A.S.*, **187**, 76p.
Stockman, H.S. *et al.* 1981, *IAU Circular No. 3616*.
Stone, R.P.S. 1977, *Ap. J.*, **218**, 767.
Stone, R.P.S. and Baldwin, J.A. 1981, *Cont. Cerro Tololo Inter-American Obs.*, No. 128.
Szkody, P., Liebert, J., and Panek, R.J. 1985, *Ap. J.*, **293**, 321.
Voíkhanskaya, N.F. 1985, *Pis'ma Astron. Zh.*, **11**, 916.
Watson, M.G. 1986, *The Physics of Accretion onto Compact Objects*, eds. K.O. Mason, M.G. Watson, and N.E. White (Berlin: Springer-Verlag).
Williams, R.E. and Ferguson, D.H. 1982, *Ap. J.*, **257**, 672.

R. Costero: Instituto de Astronomía, UNAM, Apartado Postal 70-264, 04510 México, D.F., México.
J.S.B. Dick and D.H.P. Jones: Royal Greenwich Observatory, Herstmonceux Castle, Hailsham, E. Sussex, BN27 1RP, England.
J. Echevarría: Instituto de Astronomía, UNAM, Apartado Postal 877, 22830 Ensenada, B.C., México.
R. Gilmozzi: Instituto di Astrofizica Spaziale, CP67, 00044 Frascati, Italy.
A. Schwarzenberg-Czerny: Astronomical Observatory, Al Ujazdowskie 4, 00-478, Warsaw, Poland.
M. Ward: Institute of Astronomy, Madingley Road, Cambridge CB3 OHA, England.